Applied Mathematics & Information Sciences
An International Journal

A Computer Aided Pulmonary Nodule Detection System Using Multiple Massive Training SVMs

Zhenghao Shi[1], *Minghua Zhao*[1], *Lifeng He*[4], *Yinghui Wang*[1], *Ming Zhang*[2] *and Kenji Suzuki*[3]

[1]School of Computer Science and Engineering, Xi'an University of Technology, Xi'an Shaanxi 710048, China
[2]First Affiliated Hospital of School of Medicine,Xi'an Jiaotong University, Xi'an Shaanxi 710061, China
[3]Department of Radiology,University of Chicago, Chicago, IL 60637, USA
[4]School of Information Science and Technology, Aichi Prefectural University, Nagakute, Aichi 480-1198, Japan

Received: 5 Oct. 2012, Revised: 29 Jan. 2013, Accepted: 21 Feb. 2013
Published online: 1 May 2013

Abstract: A computer aided pulmonary nodule detection system for chest radiography is proposed. The system consists of three models, viz., lung segmentation, lung nodule candidates detection and false positive reduction. Several innovations are offered in this system. The first one is that the detection of potential lung nodule candidates is conceived as a filtering process that searches for any region which has a spherical structure (where a potential nodule may happen to occur) in a chest radiograph by analysis eignvalues of Hessian matrix of an image. The second one is that a novel two stage classifier based method is developed to address the problem of false positive reduction in lung nodule detection, in which a rules based classifier is followed by a filter termed as multiple massive training supported vector machine (MTSVM), where the rules based classifier is employed to quickly remove obvious FP (outliers) so that their influence on the training of MTSVM was eliminated, the MTSVM is developed to further separate nodules from nonnodule candidates. Experimental results suggest that the proposed CAD scheme was superior to others in FPs reduction of lung nodule detection in chest radiography.

Keywords: Computer-Aided Diagnosis, Multiple Massive Training SVMs,Pulmonary Nodule Detection, Eigenvalue.

1. Introduction

Lung cancer accounts for the most cancer related deaths around the world. According to the National Cancer Institute, 213 380 new cases are expected in 2011[1]. Early detection of potentially cancerous pulmonary nodules may be a way to improve a patient's chances for survival[2]. Chest radiography is the most commonly used diagnosis technique for detection of pulmonary nodules due to its economical price and lower radiation dose in routinely examination [4]. However, detection of pulmonary nodules in chest radiography image is very challenging, it has been reported that radiologists can fail to detect pulmonary nodules on chest radiographs as many as 30% of positive cases [5].The difficulties for detecting lung nodules in radiographs are three fold: (1) There is a wide range in nodule sizes: Commonly a nodule diameter can take any value between a few millimeters up to several centimeters. (2) Nodules exhibit a large variation in density and hence visibility on a radiograph (some nodules are only slightly denser than the surrounding lung tissue, while the densest ones are calcified). (3) Nodules can appear anywhere in the lung field, and can be obscured by ribs and structures below the diaphragm, resulting in a large variation of contrast to the background.Computer-aided detection (CAD) system is considered to be a helpful diagnostic tool to handle problems mentioned above and therefore, in the past decades, various image processing methods [3] and CAD schemes have been proposed [4]. Giger et al.[6]obtained nodules using multiple grey level thresholds and rule-based approach. Xu et al.[7] described a system which utilizes a set of decision rules and a feed forward NN to find nodular patterns. Penedo et al.[8] set up two Neural Networks (NNs), with the first one detecting the suspected areas, and the second one acting as a classifier. Lee et al. [9] proposed an improved template-matching technique based on genetic algorithm template matching for detecting nodules existing within the lung area. Shiraishi et al. [10] used a localized search method based

* Corresponding author e-mail: ylshi@xaut.edu.cn, suzuki@uchicago.edu

on anatomical classification to detect nodule candidates in chest radiographs and employed a total of 71 image features for three sequential artificial neural networks in order to reduce the number of false-positive candidates. Recently, Gori et al. [11] have proposed a dot-enhancement filter for nodule candidate selection and a neural classifier for FP reduction. Hardie et al. [12] have also recently proposed a CAD system for identifying lung nodules in chest radiographs that consists of using a weighted mean convergence index detector and an adaptive distance-based threshold algorithm to segment the detected nodule candidates.

Despite much effort being devoted to, lung CAD systems remain an ongoing research topic.One of a major problem with current existing CAD schemes is a relatively large number of false positives, which is likely to lower radiologists' efficiency in using a CAD scheme[4]. Therefore, it is important to reduce the number of false positives (FPs) as much as possible while a high sensitivity is maintained. With this in mind, this paper describes a new CAD system. This new system has several novel aspects. Firstly, a computationally simple double localizing region-based active model is used for lung segmentation. Secondly, detection of lung nodule candidates is conceived as a filtering process that searches for any region with a spherical structure (where a potential nodule may happen to occur) on a chest radiograph by analysis of eignvalues of Hessian matrix. Finally, Multiple Massive Training SVMs (MTSVM) classifier is proposed for FPs reduction, which is not only computationally simple, but also has the ability to generalize well even with relatively few training samples.

The rest of the paper is organized as follows. In Section 2 The architecture of the CAD system and its modules is described. Experimental results are shown in Section 3. Analysis and discussion on experiment are given in Section 4. we present conclusions and thoughts for future improvements and work in Section 5.

2. Methodology

Figure 1 shows the block diagram of the proposed CAD system, it comprises the following modules that are processed consecutively: 1) lung segmentation; 2) multi-scale dot enhancement and lung nodule candidate generation using eigenvalues of an image Hessian matrix; 3) false positive reduction and 4) presenting CAD findings to a physician for review. This block diagram is fairly conventional. However, we believe that the novelty of our system lies in the specific choice and design of its modules. In the following sections, we will describe design of each module in detail.

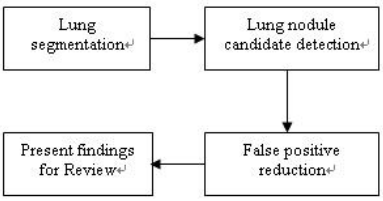

Figure 1 The diagram of the proposed CAD system

2.1. Lung Segmentation

To eliminate false positives that might occur outside of the lung, it is important to obtain a very accurate segmentation of the lung boundaries. In this work, a double localizing region-based active model[13] is employed for segmentation of lung field in chest radiographs. The basic steps of this method is described as bellows.

Firstly, we use a self-adaptive thresholding technique to categorize the image into three parts: visible lung, air and other human tissue.

Next, by fitting the average locations of the midpoint of left and right ribcage edge to a straight line using least square solution, the midline of lung area is determined.

Then double localizing regions are defined and initialized based on the parameter of midline of lung area. Here, the local region descriptors are region descriptors with probability distributions computed from feature samples within regions that lie inside windows centered on an active contour. An active contour is a deformable continuous curve whose shape is controlled by internal forces and external forceswhere internal forces act as a smoothness constraint, and external forces guide the active contour towards image features. Each pixel on the contour is considered separately, and move to minimize the energy computed in its own local region. Let $\nu(s) = (x(s), y(s))$ be the parametric description of a snake($s \in [0, 1]$). Its total energy can be written as:

$$E_{snake}(V) = \int_0^1 (E_{Int}(V(s)) + E_{Ext}(V(s)))ds \qquad (1)$$

with

$$E_{Int}(V(s)) = \frac{1}{2}[\alpha(s)|\frac{\partial(V)}{\partial(s)}|^2 + \beta(s)|\frac{\partial^2(V)}{\partial^2(s)}|^2] \qquad (2)$$

and

$$E_{Ext}(x, y) = -|\nabla X(x, y)|^2 \qquad (3)$$

where α and β are weighting parameters that control the snake's tension and rigidity, respectively. The external force of this active model is a Gaussian function. The Gaussian potential energy strength relies on the picture edge, and its shortcoming is the small action sphere where the contour must establish close to its boundary. Problems associated with initialization and poor

convergences to boundary concavities have limited their utility. Meanwhile, in the conventional active contours model, the contour curve is represented by level sets. In the level set framework, the contour curve is embedded in a higher-dimensional function, termed as signed distance function (SDF). In this form, with the contour changes, a large of computation is needed to keep up with its corresponding SDF. Aim at problems mentioned above, we use a sparse field method instead of the level set method which frequently used in conventional snake models. The sparse filed method uses an approximation to the distance transform, and this makes it feasible to re-compute the neighborhood of the level set model at each step, where key point list is employed to track the points closing to the zero level set (only one point wide). These lists are implemented as doubly-linked-lists. The properties that elements can be added dynamically into the point list, and the elements can be removed from the middle of the list.

And next then the double snake contours are employed to capture the boundary of the left and right lung. During the process of the curve capturing the lung boundary,energy of each one of the two snakes curve are minimized.The energies optimization is done by fitting a model to each local region. And at last, the boundary of two lung lobes is captured.

In respect to current existing methods, the proposed method makes no assumption regarding the chest position, size and orientation, and also much more efficient to alter the statistics based on the movement of a few points that cross the interface than to re-compute the means inside and outside of the contour at each times.

Figure.2 shows a typical image of the final segmented lung using the double localizing region-based active model. The subsequent nodule detection is calculated within the segmented lung mask.

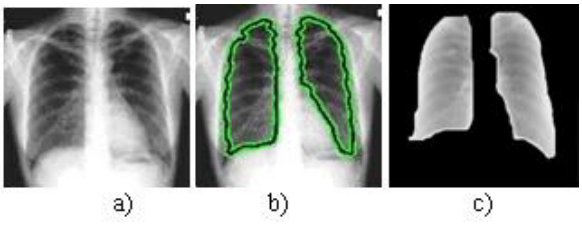

Figure 2 An example of the final segmented lung image. a) Original Chest radiography ; b) double localizing region-based snake model segmentation result; c) finally segmented lungs.

2.2. Potential nodule candidate detection

Given the fact that a nodule is generally either spherical or has local spherical elements, while a blood vessel is usually oblong. The eignvalues of Hessian matrix of an image, which provides information about the shape of the considered region, can be used as a tool to identify any region which has a spherical structure (where a potential nodule may happen to occur) in a chest radiograph.

Assume that a pixel in a 2-D image is denoted by I(x,y),and its four second derivatives are represented by I_{xx},I_{xy},$I_{yx}$and I_{yy},where $I_{xy} = I_{yx}$.Then the Hessian matrix H of the pixel I(x,y)in the original 2-D image can be constructed as [14]:

$$H = \begin{vmatrix} I_{xx} & I_{yx} \\ I_{xy} & I_{yy} \end{vmatrix} \tag{4}$$

Let λ_1 and λ_2 ($|\lambda_1| \geq |\lambda_2|$),which can calculated through the following equation, be the eigenvalues of the Hessian matrix H

$$\nabla(H - E * \lambda) = 0 \tag{5}$$

where E is the identity matrix and λ is the set of λ_1 and λ_2,which gives information about the shape of the considered region. In 2D case,λ_1 and λ_2 satisfy the following condition:

$$Blob : \lambda_1 = \lambda_2 \ll 0 \tag{6}$$

$$Line : \lambda_1 \ll 0 and \lambda_2 = 0 \tag{7}$$

Let $R_\sigma^\lambda = \frac{|\lambda_2|}{|\lambda_1|} e^{-\frac{R_c^2}{2}}$ with $R_c = k - 2\sigma$ be be the ratio for distinguishing between blob-like and line-like structures. Apparently, R_σ^λ has a value of 1 for a blob, a value of 0 for a line, and a value between 0 and 1 for a quasi-blob. In this study, we assume that the detected object is bright with respect to its background. We also refer to clusters of blobs as potential nodule concentration regions.

Because nodules in chest radiography can appear in different size, for preventing the lost detection of the positive nodules, also to reduce the second derivatives sensitivity to image noise, Gaussian kernels with a variety of scales is convolved with an image before the calculation of Hessian matrix. The Gaussian kernel for 2-D images is defined as:

$$G(x, y, \sigma) = \frac{1}{2\pi\sigma^2} exp(-\frac{x^2 + y^2}{2\sigma^2}) \tag{8}$$

where σ is standard deviation of the Gaussian kernel,it controls the scale and the smoothing effect. For nodule enhancement, this value should be fitted to the nodule density distribution. Assuming that the diameters of nodules to be enhanced are in a range of $[d_0, d_1]$ (e.g.$[2mm, 20mm]$). the N discrete smoothing scales σ_N in the range of $[\frac{d_0}{4}, \frac{d_1}{4}]$can be calculated as:

$$\sigma_1 = \frac{d_0}{4}, \sigma_2 = r\sigma_1, ..., \sigma_N = r^{N-1}\sigma_1 = \frac{d_1}{4} \tag{9}$$

where

$$r = (\frac{d_1}{d_0}^{\frac{1}{N-1}}) \tag{10}$$

To find the right diameter of a blob in chest radiography, R_σ^λ is analyzed at different scale.The algorithm starts at an area of interest with a kernel with the smallest scale for the convolution. Then the scale value is incrementally extended. For every kernel size the eigenvalues are calculated. Finally, values of R_σ^λ at different scales are fused to obtain the final measure of blob likeness. For the best fitting kernel size the ratio of R_σ^λ has the highest value at one scale. This means that the detection can be stopped if the value of the classifier R_σ^λ begins to decrease, and at which the Gaussian kernel will approximately matches the size of the blob to be detected. The maximum response R_{max}^λ can be written as

$$R_{max}^\lambda = max(R_\sigma^\lambda), \sigma \in [\sigma_{min}, \sigma_{max}] \tag{11}$$

The detected blob point $I_B(x, y)$ can be expressed as

$$I_B(x,y) = \{ \begin{matrix} 1 : if R_{max}^\lambda \\ 0 : others \end{matrix} \tag{12}$$

By apply above mentioned method to a database of 60 radiographs (30 nodules), we identified 724 nodule candidates that included 24 nodules and 700 false positive detections. Figure 3 shows an example of the potential nodule detection result with above mentioned method. Detection of lung nodule candidates is indicated by white circles. In this study, a relaxed threshold level was used, so that 18-20 false positive detections per image were produced by the CAD scheme.

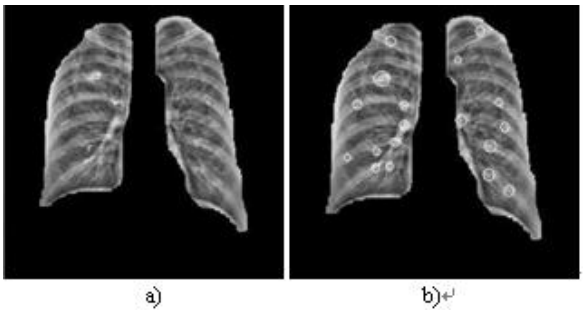

Figure 3 An example of detection of lung nodule candidates using eigenvalues of Hessian matrix. a) Input image ; b) detected nodule candidates

2.3. False positive reduction

In this section, a two stage classifier method is developed to address the problem of false positive reduction in lung nodule detection. Firstly, a rule-based classifier is employed to quickly remove obvious FP (outliers) so that their influence on the training of the second classifier was eliminated. Then a filter termed as multiple massive training supported vector machine (MTSVM) is developed to further separate nodules from nonnodule candidates; both described below.

For rule-based classifier, two features, viz., sphericity and effective diameter, were used. Each feature is associated with one rule. The output from one rule will be employed as the input to a subsequent rule. Here the sphericity is defined by R_σ^λ. We take a spherical region as a nodule with

$$R_\sigma^\lambda \geq \vartheta \tag{13}$$

where $\vartheta$is the high shape index threshold chosen experimentally. The sphericity can be used to remove the object that is elongated.

The effective diameter is defined as the diameter of circle with the same area of the initial detected region of interest(ROI). This feature is used to remove very small nodule candidates.

Motivated by [15], MTSVM is developed to further separate nodules from nonodules, where the distribution of each class is estimated separately to avoid inter-class influence. Figure 4 shows the architecture of MTSVM. It consists of four non-linear SVMs arranged in parallel and one neural network arranged in serial. Based on the structural risk minimization principle, a non-linear SVM classifier seek to construct a hyper-plane in the feature space as the decision surface so that the margin of separation between two classes is maximized and the error rate in the sample space is bounded to a certain upper limit[16]. That guarantees theoretically the largest generalization ability of a SVM model. When designing SVM classifier, the kernel used for feature mapping has to be chosen carefully since an inappropriate kernel can lead to poor performance. In our experiment, we use Gaussian radial basis kernel function.

The inputs to each SVM of the above four SVMs are pixel values in a sub-region of the region of interest (ROI). The output of each such SVM is a continuous value that corresponds to the center pixel in the sub-region, represented by

$$f(x,y) = K\{g(x-i, y-i) | i, j \in R_s\} \tag{14}$$

where f(x,y) denotes an estimate for the teaching value,x and y are the indices of coordinates,K{•} is the kernel of the SVM classifier, g(x,y) is a normalized input pixel value, and R_s is the local window of the SVM.

The training for each of above individual non-linear SVM is implemented by use of a large number of sub-regions obtained by scanning pixel by pixel over a training region in an input image together with teacher images. The teaching images here are produced with the following 2D Gaussian function:

$$f_\sigma(\sigma, x, y) = \frac{1}{2\pi\sigma^2} e^{-\frac{x^2+y^2}{2\sigma^2}} \tag{15}$$

where σ is the standard deviation. The distinction between a nodule and a non-nodule is determined by use of a score defined from the output images of the trained

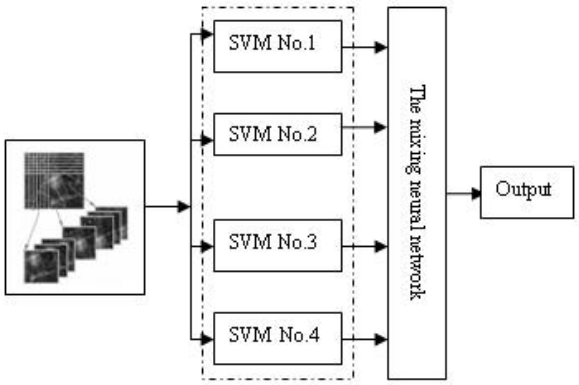

Figure 4 Architecture of the multiple mass training SVMs employed for distinction between nodules and non-nodules in this study. Each SVM classifier arranged in parallel is trained by use of a same set of typical nodules and a different set of typical non-nodules. Each of them acts as an expert for distinguishing nodules from a specific kind of non-nodules. The outputs of all SVMs are combined by use of a mixing ANN.

non-linear SVMs and a 2D Gaussian weighting function, as shown in the following Equation:

$$S_{ns} = \sum f_\sigma(\sigma_n, x, y) \times f_{ns}(x, y), (x, y) \in R_E \qquad (16)$$

where S_{ns} is the score of the nth trained SVM for the s^{th} nodule candidate,R_E is the region for evaluation, $f_{ns}(x, y)$is the output image of the nth trained SVM for the s^{th} nodule candidate where its center corresponds to the center of R_E, $f_\sigma(\sigma_n, x, y)$ is a two dimensional Gaussian function with standard deviation σ_n, where its center corresponds to the center of R_E and n is the SVM number in the multiple SVMs.This score represents the weighted sum of the estimate for the likelihood of the image containing a nodule near the center, i.e., a higher score would indicate a nodule, and a lower score would indicate a non-nodule.

To remove all major sources of FPs, the outputs of above four single non-linear SVMs are combined with a mixing ANN. The mixing ANN consists of a modified three layer ANN with a modified BP training algorithm for processing continuous output values. The activation functions of the units in the input, hidden, and output layers are an identity, a sigmoid, and a linear function, respectively. After training of the mixing ANN, the mixing ANN is expected to output a value related to the "likelihood of nodule", i.e., a higher value for a nodule, and a lower value for a non-nodule. By thresholding of the output, a distinction between a nodule and a non-nodule can be made.

Referred the parameters used in [15],in this study, the size of the sub region R_s, the standard deviation of the 2D Gaussian distribution, and the size of the training region in the teaching image were determined empirically to be 9×9 pixels, 5.0 pixels, and 19×19 pixels, respectively. About the mixing neural network, in this study, the numbers of units in the input, hidden, and output layers were 8, 7, and 1, respectively. The slope of the linear function of the output unit and the learning rate were 0.1 and 0.1, respectively.

Figure 5 shows an example of input images and corresponding output images for MTSVMs. As shown in Fig.5a), the output images of the trained MTSVMs for nodules are represented by light distributions. The output images for non-nodules are relatively dark around the center, as shown in Fig. 5b)

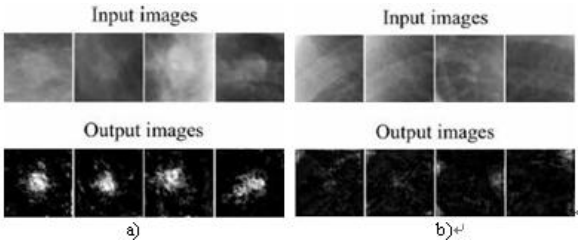

Figure 5 A distinction between a nodule and a non-nodule using MTSVMs. a) images with nodules; b) images without nodules

3. Experimental Results

In this section, we present a number of experimental results to demonstrate the efficacy of the proposed CAD system. We begin by present results for the nodule candidate detector. We then present the overall system performance results. Finally, we compare the performance of the proposed CAD system with that of other reported systems.

3.1. Material

The database used in this study consisted of 60 posterior anterior chest radiographs selected from the Japanese Standard Digital Image (JSRT) Database 13 developed by the Japanese Society of Radiological Technology, which is available publicly. The JSRT Database includes 154 abnormal chest radiographs, each with a solitary pulmonary nodule, and 93 non-nodule chest radiographs. These original screen-film images were digitized with a 0.175 mm pixel size, matrix size of 20482048 pixels, and 12 bits of gray scale. For computational efficiency, the size of the chest radiographs was reduced by a factor of 4 to 440440 pixels with a 12 bit grey scale level by use of averaging. The absence and presence of nodules in the chest radiographs were confirmed by use of CT examinations. The ground truth used in this study was established by use of CT examinations.

3.2. Potential nodule detection performance

In this subsection, we evaluate the performance of the Hessian matrix candidate detector. We compare the sensitivity of the Hessian matrix candidate detector with that of the LoG based candidate detector. The sensitivity is defined as:

$$Sensitivity = \frac{TP}{TP + FN} \quad (17)$$

where TP is the number of true positive nodules (the part of the image is correctly classified as nodule), FN is the number of false negative nodules (the part of the image is incorrectly classified as background). The comparison results are shown in table 1.

As it can be seen from table 1 that LoG detector has a sensitivity of 83% with 15 detections per image, and Hessian matrix based detector has a sensitivity of 85% with 12 detections per image. With comparable sensitivity, the Hessian based detector has 20% greater specificity (i.e.,12 detections per image versus 15).

Table 1 The Comparison of the Hessian Matrix Candidate Detector and the LoG Based Candidate Detector

Performance	Hessian detector	LoG detector
Sensitivity	85%	83%
False positive	12	15

3.3. Overall system performance

The overall system performance is quantified by a comparison of the proposed CAD scheme with individual SVM classifier based CAD scheme and a Fisher linear discriminant (FLD) classifier based CAD scheme [17] using the free response receiver operating characteristic (FROC) curves. The FROC curve express an overall sensitivity as a function of the number of false positives per image at a specific operating point on the curve. The FLD classifier is a typical widely used classifier in CAD scheme for lung nodule detection [17].

Figure 6 shows the experimental results. From figure 6, it can be seen that the overall sensitive of the proposed CAD scheme can approach to 85% while that of an individual SVM based CAD scheme and a FLD classifier based CAD scheme can only approach to 83% and 81%, respectively. It can also be noticed that, with the proposed CAD system, at an overall sensitivity of 85%, the false positive was reduced from 12 to 4 positives per image. However, with an individual SVM based CAD scheme or a FLD classifier based CAD scheme, the false positive was only reduced from 12 to 6 per image at an overall sensitivity of 83% and of 81%, respectively. These results suggest that the proposed scheme was superior to others in FPs reduction in lung nodule detection on chest radiograph.

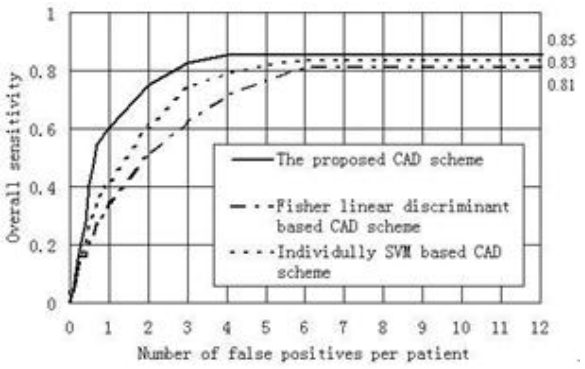

Figure 6 Evaluation of overall system performance by a comparison of the proposed CAD scheme with individual SVM classifier based CAD scheme and a Fisher linear discriminant (FLD) classifier based CAD scheme using the free response receiver operating characteristic (FROC) curves.

4. Discussion and Conclusion

In this paper, a new CAD system for the detection of lung nodules in chest radiography based on rules based classifier and Multiple Massive Training SVMs is presented. The paper describes the complete design of the CAD system and presents a detailed performance analysis on the publicly available JRST database.

The proposed system offers several useful innovations. The double localizing region-based active model algorithm used for lung segmentation is attractive because it is conceptually and computationally simple. We believe that conceiving the detection of lung nodule candidates as a filtering process that searches for any region which has a spherical structure (where a potential nodule may happen to occur) in a chest radiograph and using eignvalues based Hessian matrix do such a work is very useful for improve the sensitive of lung nodule detection.

The majority of false positive detections eliminated by the MTSVMs were not included in the training data set. Therefore, the experiments results suggest that the MTSVM could be a useful tool in eliminating false positive detections in CAD scheme for detection of lung nodules in chest images. It is not only computationally simple, but it also has the ability to generalize well even with relatively few training samples. The performance of the MTSVMs appeared to supass that of an individually SVM and an individually FLD in distinguishing nodules from false positive detections.

As mentioned previous, one advantage of the local shape feature is that it characterizes the local geometric feature and favors regions with high spherical elements. This is the main reason that the proposed algorithm is able to detect not only spherical nodules, but also

non-spherical nodules with aspects of high local spherical elements.

Although the proposed CAD system appears promising, further optimization of the different module parameters could improve the overall performance of the CAD system. More anatomical context features may also help to improve the overall system performance by targeting certain classes of observed FPs.

Acknowledgement

This work is partially supported by a grant from the Nature Creative Science Program of BeiLin Science committee (No.GX1213), the Nature Creative Science Program of Xi'an University of Technology (No.211107) and the National Natural Science Foundation of China (No.61072151). The authors also gratefully acknowledge the helpful comments and suggestions of the reviewers.

References

[1] A. Jemal,R. Siegel,J.Q. Xu, and E.Ward, CA Cancer J Clin **60**, 277 (2010).
[2] K. Doi, Computerized Medical Imaging and Graphics **31**, 198 (2007).
[3] Z. Qu, Appl. Math. Inf. Sci. **6**, 105s (2012).
[4] B.V.Ginneken, Bart M. ter Haar Romeny, and Max A. Viergever, IEEE Transactions on medical imaging **20**, 1228 (2001).
[5] R.C. Hardie , S.K. Rogers, T.Wilson and A.Rogers, Medical Image Analysis **12**, 240 (2008).
[6] M.L.Giger, K.T.Bae, H.MacMahon, Invest Radiol. **29**, 459 (1994).
[7] X.W.Xu, K.Doi, T.Kobayashi, H.MacMahon, M.L.Giger, Med Phys. **24**, 1395 (1997).
[8] M.G.Penedo, M.J. Carreira, A.Mosquera and D.Cabello, IEEE Trans. Med. Imag. **17**, 872 (1998).
[9] Y. Lee, T. Hara, H. Fujita, S. Itoh and T. Ishigaki, IEEE Trans. Med. Imag. **20**, 595 (2001).
[10] J. Shiraishi, F. Li and K. Doi, Acad. Radiol. **14**, 28 (2007).
[11] I. Gori, M.Fantacci, A. Preite Martinez, A.Retico, Proc. of the SPIE on Medical Imaging 2007: Computer-Aided Diagnosis,Maryellen, L., Karssemeijer, Nico (Eds.), 6514 (2007).
[12] R. Hardie, S. Rogers, T. Wilson and A. Rogers, Proc. Medical Image Analysis **12**, 240 (2008).
[13] Z.H. Shi, L. Li, H. Wang, F. Wang, M. Zhao, Y. Wang, Q. Yao, ICIC Express Letter, PartB:Application **2**, 69 (2011).
[14] Q. Li, S.Sone and K.Doi, Med. Phys.**30**, 2040 (2003).
[15] K.Suzuki,J.Shiraishi,H.Abe, H.MacMahon, and K.Doi, Academic Radiology **12**, 191 (2005).
[16] C.C. Change and C.J.Lin, www.csiew.ntu.edu.tw/ cjlin/libsvm.
[17] M.Temesguen, R. C. Hardie and S. K. Rogers, Medical Image Analysis **14**, 390 (2010).

Zhenghao Shi received the BS degree in material science and engineering from Dalian Jiaotong University, Dalian,China, in 1995, the MS degree in computer application technology from Xi'an University of Technology,Xi'an, China, in 2000, and the Ph.D degree in computer architecture from Xi'an institute of microelectronics, Xi'an, China, in 2005. In 2000, he joined Xi'an University of Technology, Xi'an, China. From 2000 to 2005, he was a assistant professor in the department of computer science and engineering at Xi'an University of Technology. From 2006 to now, he is an associate professor of the department of computer science and engineering at the same University. During the period of 2006 to 2007, of 2008 to 2009, he was on leave with the department of computer science and engineering at Nagoya institute of technology, Nagoya, Japan, for image research as a postdoctral researcher, respectively. From 2007 to 2008, he was a research associate in the Kurt Rossmann Laboratories for Radiologic Image Research, the Department of Radiology, the Division of Biological Sciences, the University of Chicago. His research interests include neural networks for image processing and pattern recognition, computer-aided diagnosis, and image processing suggested by the human visual systems. He is a member of the IEEE, also a member of ACM.

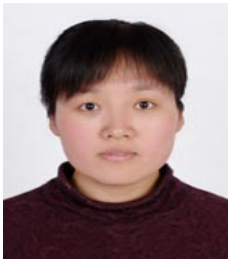

Minghua Zhao received her Ph.D degree in computer science from Sichuan University, Chengdu, China, in 2006. After that, she joined Xi'an University of Technology, Xi'an, China. Currently, she is an associate professor of the department of computer science and engineering at the same University. Her research interests include image processing and pattern recognition.

Lifeng He received the B.E. degree from the Northwest Institute of Light Industry, China, in 1982, and the M.S. and Ph.D. degrees computer science from Nagoya Institute of Technology, Japan, in 1994 and 1997, respectively. He is an associate professor at the Aichi Prefectural University, Japan, and a guest professor at the Shaanxi University of Science and Technology, China. From September 2006 to May 2007, he worked at the University of Chicago (USA) as a research associate. His research interests include image processing, automated reasoning, and artificial intelligence.

Yinghui Wang received the Ph.D. degrees from the Northwest University, China, in 2002. Currently, He is an professor at Xi'an University of Technology, China. From September 2003 to May 2005, he worked at peiki University as a research associate. His research interests include image processing and artificial intelligence.

Ming Zhang received the BS,the MS degrees and the PhD degree in radiography from medical college at Xi'an Jiaotong University, China,in 1989,1997 and 2000, respectively. Since 1989,he has been a faculty of the Department of Radiology, the Division of medical, Xi'an Jiaotong University Currently, he is a professor of the same university. His research interests include computer-aided diagnosis, and magnetic resonance imaging on the central nervous system.

Kenji Suzuki received the BS and MS degrees, both with highest honors, in electrical and electronic engineering from Meijo University, Nagoya, Japan, in 1991 and 1993, respectively, and the PhD degree in information engineering by a thesis from Nagoya University, Nagoya, Japan, in 2001. From 1993 to 1997, he was with the Research and Development Center at Hitachi Medical Corporation, Kashiwa, Japan, as a researcher. He was engaged in research and development of intelligent medical imaging systems, including a digital angiography system and a digital radiography system. In 1997, he joined Aichi Prefectural University, Aichi, Japan, where he assisted on founding the Faculty of Information Science and Technology. From 1998 to 2002, he was a research associate in the Faculty of Information Science and Technology at Aichi Prefectural University. During the period of 2001 to 2002, he wason leave with the KurtRossmannLaboratories for Radiologic Image Research, the Department of Radiology, the Division of Biological Sciences, The University of Chicago, Illinois, as a research associate. From 2002 to 2003, he was a research associate in the Kurt Rossmann Laboratories for Radiologic Image Research, the Department of Radiology, the Division of Biological Sciences, the University of Chicago. Since 2003, he has been a research assiciate (instructor) at the same university. He received the Paul C. Hodges Award from the Department of Radiology, The University of Chicago in 2002. He was a member of the research group organized by the Aichi Science and Technology Foundation, Japan, from 1997 to 1998. He was an investigator of the research project promoted by the Ministry of Education, Science, Sports, and Culture of Japan, Quantum Information Theoretical Approach to Life Science, in the Frontiers of Science and Technology at Meijo University from 1997 to 2002. His research interests include neural networks for image processing and pattern recognition, computer-aided diagnosis, and image processing suggested by the human visual systems. He is a member of the IEEE, IEICE, IEEJ, IPSJ, JNNS, and JCS.